Thermal Characteristics of a Multichip Module Using PF-5060 and Water

Mingoo Choi* and Keumnam Cho**

(Received October 30, 1998)

The experiments were performed by using PF-5060 and water to investigate the thermal characteristics from an in-line 6×1 array of discrete heat sources for simulating the multichip module which were flush mounted on the top wall of a horizontal, rectangular channel of aspect ratio 0.2. The inlet temperature was 15℃ for all experiments, and the parameters were the heat flux of simulated VLSI chips with 10, 20, 30, and 40W/cm² and the Reynolds numbers ranging from 3,000 to 20,000. The measured friction factors for PF-5060 and water gave a good agreement with the values predicted by the modified Blasius equation within ±6%. The chip surface temperatures for water were lower by 14.4~21.5℃ than those for PF-5060 at the heat flux of 30W/cm². From the boiling curve of PF-5060, the temperature overshoot at the first heater was 3.5℃ and was 2.6℃ at the sixth heater. The local heat transfer coefficients for water were larger by 5.5~11.2% than those for PF-5060 at the heat flux of 30W/cm², and the local heat transfer coefficients for PF-5060 and water reached a uniform value after the fourth row. This meant that the thermally fully developed condition was reached after the fourth row. The local Nusselt number data gave the best agreement with the values predicted by the Malina and Sparrow's correlation and the empirical correlations for Nusselt number were provided at the first, fourth and sixth rows for a channel Reynolds number over 3,000.

Key Words: Multichip Module, Rectangular Channel, Modified Blasius Equation, Heat Transfer Coefficient, Nusselt Number

Nomenclature

A : Surface area (m^2)
C_p : Specific heat at constant pressure (kJ/kg · K)
D_h : Hydraulic diameter (m)
f : Fanning friction factor
h : Heat transfer coefficient (W/m² · K)
k : Thermal conductivity (W/m · K)
L : Length (m)
Nu : Nusselt number (=h · Dh/kf)
P : Pressure (Pa)
Pr : Prandtl number ($=\mu f \cdot Cp/kf$)
q″ : Heat flux (W/cm²)
R : Resistance (Ohm)
Re : Reynolds number ($=\rho_f \cdot U \cdot D_h/\mu_f$)
T : Temperature (℃)
U : Average velocity (m/s)
V : Voltage (V)

Greek Letters

δ : Uncertainty
μ : Viscosity (N · s/m²)
ρ : Density (kg/m³)

Subscripts

f : Working fluid
i : Inlet of the test section
s : Chip
sat : Saturation
sub : Subcooling
w : Water

* School of Mechanical Engineering, Graduate School, Sung Kyun Kwan University, Suwon, Korea
** School of Mechanical Engineering, Sung Kyun Kwan University, Suwon, Korea

1. Introduction

The increase in circuit density forced the printed circuit board(PCB) technology to give way to the surface mounted technology (SMT). Surface mounted assemblies dominated the system packaging approach back in 1980s. However, continuing progress of more complex and dense VLSI chips made even the SMTs inefficient and have led to the development of a new packaging approach called the multichip modules (MCMs). MCMs offer several advantages such as reduced weight, reduced size, increased reliability and enhanced performance. As the packaging density increases for a multichip module, an efficient cooling method is required. The heat flux should be removed within the ranges of 50~100W/cm^2 for a single chip and up to 25W/cm^2 for multichip module (Nakayama, 1997 ; Incropera, 1988 ; Bar-Cohen, 1994, 1997). A direct liquid cooling method using fluorocarbon has been used for the cooling of multichip modules. Fluorocarbon is electrically insulating and chemically stable. The direct liquid cooling method using fluorocarbon is classified as the forced convection cooling method (Baker, 1972 ; Incropera et al. 1986), pool boiling cooling method (Park and Bergles, 1987; Mudawar and Anderson, 1990), forced convection boiling cooling method (Mudawar and Maddox, 1990; Heindel et al., 1992). However, the direct liquid cooling method is recently replaced by the indirect liquid cooling method due to both the maintenance problem of the system and the thermal shock produced by thermal hysteresis.

Therefore, the present study is primarily concerned with measuring the convective heat transfer data for a linear array of square heat sources with high heat flux which plays the role of a MCM, cooled by the indirect liquid cooling method. Experimental results are compared with the existing correlations under continuous heating condition, and the new correlations under discrete heating condition are provided.

2. Experimental Apparatus and Procedure

Present experiments were performed with water and PF-5060 (a dielectric liquid manufactured by 3M Co.). PF-5060 is an alternative coolant of FC-72, and its typical properties are shown and compared with FC-72 and water in Table 1.

The schematic diagram of the experimental apparatus is shown in Fig. 1. The apparatus consisted of a main test section, a constant temperature bath, a power supply, a mass flow meter, a pump, a data acquisition system etc. The test section consisted of a rectangular channel and a multichip module.

The rectangular channel with an aspect ratio of 0.2 shows the most efficient cooling performance for a fully developed laminar single phase flow in the case of the heated top wall with uniform heat flux (Hartnett and Kostic, 1989). Since the present study deals with a fully developed turbulent flow and discrete heating at the top wall, results reported in the literature cannot directly be applied to the present study. Since no data on the aspect ratio were reported for the fully developed turbulent flow, an aspect ratio of 0.2 (7.6 ± 0.05mm $\times$ 38.1 ± 0.05mm) was chosen. The hydraulic diameter of the rectangular channel was 1.26cm.

The multichip module had an in-line 6×1 array of discrete heat sources simulating VLSI chips, and it was flush-mounted on the top wall of a horizontal rectangular channel. The multichip module was located at a downstream location 50 times of the hydraulic diameter from the

Table 1 Properties of the Fluorinert liquids and water (at 25℃ and 1atm)

Property	PF-5060	FC-72	water
Boiling point (℃)	56	56	100
Density (Liquid) (g/cm^3)	1.68	1.68	1.0
Viscosity (Liquid) (cs)	0.4	0.4	0.9
Surface tension (dyne/cm)	12.0	12.0	72
Vapor pressure (kPa)	30	30	3.3
Heat of vaporization (cal/g)	21	21	540
Specific heat (cal/(g · ℃))	0.23	0.25	1.0

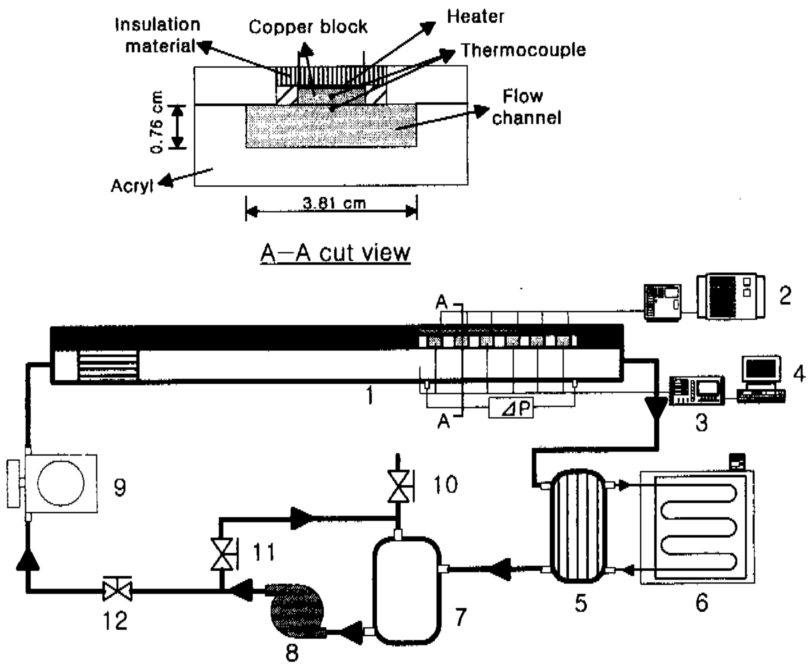

Fig. 1 Schematic diagram of the experimental apparatus.

inlet of the test section, where flow was hydrodynamically fully developed. A honeycomb section was located at the inlet of the channel to make the flow uniform. Two static pressure taps were located at the bottom wall just before and after the MCM and connected to an U-tube manometer to measure the pressure drop across the MCM. A heating wire with a resistance of 18.6$\pm$0.2Ω was attached to each chip by silicon glue for a heat source. Six heating wires on the chips were connected in parallel to a power supply with an accuracy of $\pm$0.03V to supply a uniform heat flux to each heater. Each heat source had a square shape with a size of 1.27cm, a typical size for a VLSI chip. The distance between two adjacent chips was 1.27cm. A copper heat sink with a thickness of 6mm was attached at the bottom of each chip, and the top side was thermally insulated by a fiberglass to force the heat flow only to the channel. The copper heat sink was a square shape of the same size as the heater. The maximum temperature difference at three positions on a copper heat sink was approximately 0.5℃. The temperatures of the copper heat sink and the fluid temperatures just below (0.5mm) the copper heat sink surface were measured by type T thermocouples inserted through machined holes. The thermocouples were calibrated within an accuracy of $\pm$0.15℃ by a standard RTD.

A conduction analysis was performed on the heat source and the substrate using the values of thermal conductivities for copper block (386W/m·K), acryl (0.2W/m·K), thermal silicon (1.6W/m·K), and insulation (0.02W/m·K). The heat loss from the heater to the surrounding ranged from 2.1 to 3.3% in the whole experimental range and was compensated in the calculation of heat flux on the heater.

Two key experimental parameters were the heat flux and channel Reynolds number. The heat flux varied from 10 to 40W/cm^2 and the channel Reynolds number ranged from 3,000 to 20,000. The heat flux was obtained by dividing the heat supplied to each chip by the chip area. The Reynolds number was based on the hydraulic diameter of the rectangular channel with an aspect ratio of 0.2. The inlet temperature of the test section was set to 15$\pm$0.15℃ for all runs.

3. Data Reduction and Uncertainty Analysis

The local heat transfer coefficient was calculated by dividing the heat flux supplied to each chip by the temperature difference between the surface temperature of the chip and the fluid temperature measured at a location 0.5mm below the chip as shown in Eq. (1). The heat flux is obtained using the supplied voltage and the resistance of heater as shown in Eq. (1).

$$h=\frac{q''}{T_s-T_f}=\frac{V^2}{RA_s}/(T_s-T_f) \tag{1}$$

The equations for the uncertainty analysis of the local heat transfer coefficient and the heat flux are shown in Eqs. (2) ~ (3) by following the procedure in the literature (Moffat, 1985).

$$\frac{\delta h}{h}=\sqrt{\left(\frac{\delta q''}{q''}\right)^2+\left(\frac{\delta T_s}{T_s-T_f}\right)^2+\left(\frac{\delta T_f}{T_s-T_f}\right)^2} \tag{2}$$

$$\frac{\delta q''}{q''}=\sqrt{\left(\frac{\delta R}{R}\right)^2+\left(2\frac{\delta V}{V}\right)^2+\left(2\frac{\delta L_s}{L_s}\right)^2} \tag{3}$$

The uncertainties of T_s, T_f, resistance, voltage, and the heater length (L_s) are 0.65℃, 0.15℃, 0.2Ω, 0.03V and 0.02mm, respectively, for the whole experimental range. The uncertainty of the heat flux calculated by Eq. (3) was $\pm 1.19\%$ for both PF-5060 and water, and the uncertainties of the local heat transfer coefficient by Eq. (2) were $\pm$ 3.9% for PF-5060 and $\pm 3.1\%$ for water.

4. Results and Discussion

4.1 Pressure drop and friction factor in the test section

Figure 2 shows the pressure drop and the apparent Fanning friction factor in the test section as a function of Reynolds number. Pressure drop is the difference between the static pressures in the channel before and after the MCM. The Blasius equation which supposed to predict the fully developed turbulent friction factor in smooth circular ducts was introduced by Jones (1976) for rectangular ducts. The modified Blasius equation is defined as

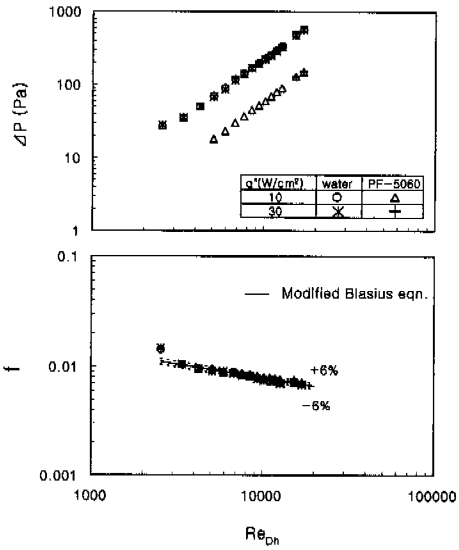

Fig. 2 Pressure drop and friction factor in the test section.

Table 2 Values of a in Eq. (5).

Aspect ratio	1	0.75	0.50	0.23	0
a	1.125	1.106	1.029	0.878	0.667

$$f=0.079\,(Re^*_{D_h})^{-0.25} \tag{4}$$

The Kozicki Reynolds number, $Re^*_{D_h}$, in Eq. (4) is given by the following expression

$$Re^*_{D_h}=a(\rho UD_h/\mu) \tag{5}$$

where the value of a in Eq. (5) depends on the aspect ratio, as shown in Table 2. The value of a for the aspect ratio 0.2 was obtained by interpolating the values of a between the aspect ratio of 0 and 0.23.

Measured friction factors for water and PF-5060 at both 10 and 30W/cm² gave a good agreement with the values predicted by the modified Blasius equation within $\pm 6\%$. As shown in Fig. 2, the pressure drop for water was approximately 4 times larger than that for PF-5060, but the apparent Fanning friction factors for water and PF-5060 showed little difference. The reason is that the pressure drop is proportional to the apparent Fanning friction factor and the square of average velocity. The average velocity for water is about twice larger than that for PF-5060 at the same Reynolds number since the kinematic viscosity for water is 2.25 times larger than that for PF-5060 as shown in Table 1.

4.2 Chip surface temperature and boiling curve

The heat flux ranges for the chips are shown in Fig. 3 with respect to the chip surface temperatures at the first and sixth rows of the multichip module at a channel Reynolds number of 20,000. For PF-5060 and water, the temperature difference between the first and sixth rows increased as the heat flux increased. The chip surface temperatures for water were lower than those for PF-5060

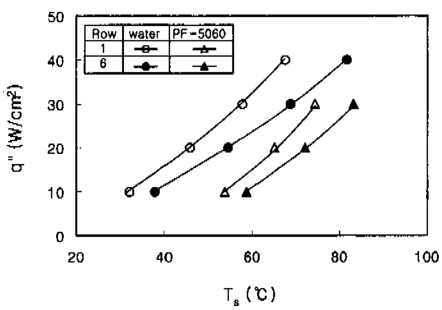

Fig. 3 Heat flux vs. surface temperature (Re_{D_h}=20, 000).

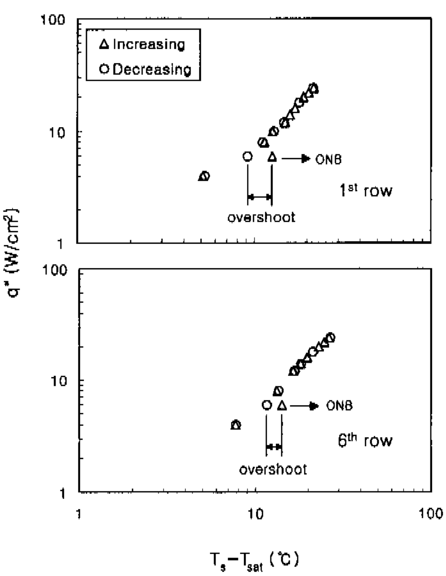

Fig. 4 Boiling curve for PF-5060 (Re_{Dh}=11,200 and ΔTsub=41℃).

since the specific heat at constant pressure for PF-5060 is approximately 25% of that for water. The chip surface temperatures for water were lower by 20.9~21.5℃ than those for PF-5060 for the heat flux of 10W/cm^2. As the heat flux increased to 30W/cm^2, the boiling at the chip surface became more active than the case with the heat flux of 10W/cm^2 and thus, the chip surface temperatures for water were lower by 14.4~16.6℃ than those for PF-5060. When the heat flux was over 40W/cm^2, the heater surface temperature for PF-5060 abruptly increased over 300℃, and the experiment became meaningless.

Boiling curve for PF-5060 is shown in Fig. 4 at the first and sixth rows for an average velocity of 0.386m/s (Re_{Dh}=11,200) at the inlet of the test section and for the case of a subcooling of 41℃. Subcooling(ΔTsub) is a temperature difference between the saturation temperature of PF-5060 (T_{sat}=56℃) and inlet temperature(T_i=15℃). At low heat fluxes below approximately 5W/cm^2, a single phase convection was a dominant heat transfer mode even though the surface temperature was over the saturation temperature. The single phase convection effect at the first heater is larger than that at the sixth heater since the sixth heater is continuously affected by other heaters. The temperature overshoot was 3.5℃ and 2.6℃ at the first and sixth heaters, respectively. The temperature overshoot is defined as the difference between the onset temperature of nucleate boiling (ONB) and the temperature obtained from the boiling curve at the same heat flux with ONB.

4.3 Local heat transfer coefficients

The local heat transfer coefficients were obtained by using the chip surface temperature and the fluid temperature just below the chip surface. Figure 5 shows the local heat transfer coefficients with respect to the row number for a channel Reynolds number of 20,000 and the heat fluxes of 10 and 30W/cm^2. The local heat transfer coefficients reached an uniform value approximately after the fourth row (seven times of the chip length). This meant that the thermally fully developed condition was reached after the fourth row. The local heat transfer coefficients for water

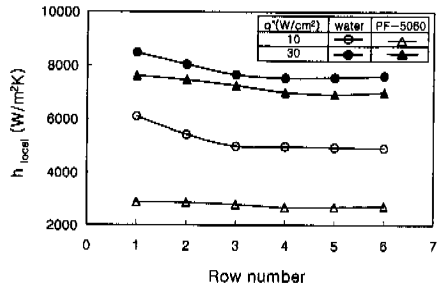

Fig. 5 Local heat transfer coefficient vs. row number (Re_{Dh}=20,000).

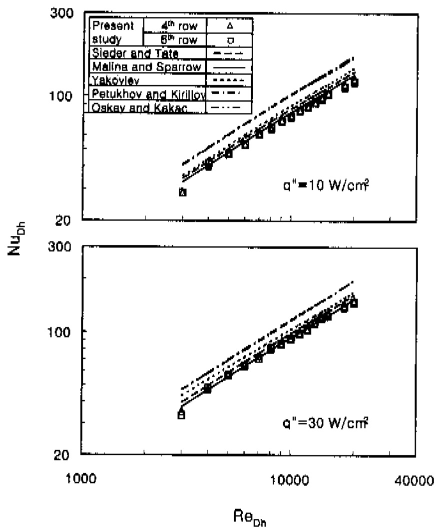

Fig. 6 Comparison of the present experimental data with the values predicted by various correlations for water.

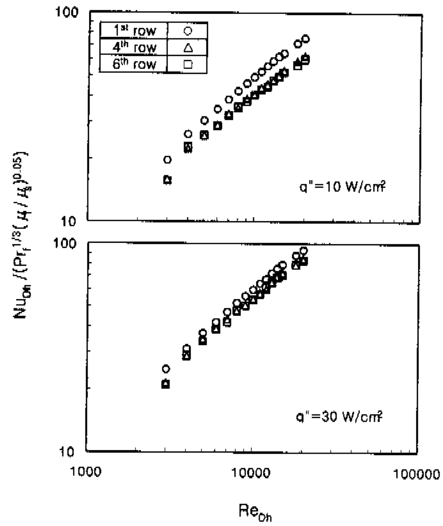

Fig. 7 Nusselt number vs. Reynolds number for water.

at the heat flux of 10W/cm^2 were about 1.7~2.1 times larger than those for PF-5060. As the heat flux increased to 30W/cm^2, the local heat transfer coefficients for water were larger only by 5.5~11.2% than those for PF-5060. The reason was that as the heat flux increased up to a certain value, a subcooled nucleate boiling near a heater surface made the local heat transfer coefficient for PF-5060 increase.

The local Nusselt numbers for water were compared with the correlations by Sieder and Tate(1936), Malina and Sparrow(1964), Yakovlev(Rogers, 1980), Petukhov and Kirillov(Petukhov, 1970), and Oskay and Kakac(1973). These correlations were on the hydrodynamically and thermally fully developed turbulent forced convection in circular ducts for liquids with variable properties.

The comparison at the fourth and sixth rows for the heat fluxes of 10 and 30W/cm^2 is shown in Fig. 6. Even though the slopes of the experimental results were slightly lower than the Malina and Sparrow's correlation, the values predicted by the Malina and Sparrow's correlation gave the best agreement with the present experimental data among the other correlations. For the heat flux of 10W/cm^2, the local Nusselt numbers of the present study were lower by 2.2~7.6% than the values predicted by the Malina and Sparrow's correlation, and for the heat flux of 30W/cm^2, the Malina and Sparrow's correlation agreed with the present experimental data within $\pm$3%.

The Nusselt numbers for the first, fourth, and sixth rows are shown in Fig. 7 with respect to the channel Reynolds number by using the viscosity ratio exponent of 0.05, and the Prandtl number exponent of 1/3. The local Nusselt numbers at the first row were 17~24% at the heat flux of 10W/cm^2, and 7~11% at the heat flux of 30W/cm^2 larger than those for the fourth row because the first row was in the thermally developing condition.

An empirical correlation was obtained at the first, fourth, and sixth rows for a channel

Table 3 Values of coefficients in Eq. (6).

Heat flux (W/cm^2)	Row No.	C	m	Maximum deviation(%)
10	1	0.107	0.665	2.6
	4	0.116	0.636	2.5
	6	0.146	0.610	2.2
30	1	0.113	0.681	2.8
	4	0.126	0.659	2.2
	6	0.123	0.661	2.4
Malina and Sparrow(1964)		0.023	0.8	

Reynolds number over 3,000. The new correlation based on the present results is provided by the following form:

$$\frac{Nu_{Dh}}{Pr_f^{1/3}(\mu_f/\mu_s)^{0.05}}=C\ Re_{Dh}^{m} \tag{6}$$

where the values of C and m are presented in Table 3 along with the maximum deviations of the data from the correlations.

5. Conclusions

The present study can be concluded as follows.

(1) The measured friction factors for both water and PF-5060 gave a good agreement with the values predicted by the modified Blasius equation within $\pm 6\%$.

(2) The chip surface temperatures for water were lower than those for PF-5060 at the heat flux of $30W/cm^2$, and from the boiling curve of PF-5060, the temperature overshoot was 3.5℃ and 2.6℃ at the first and sixth heaters.

(3) The local heat transfer coefficients for water were 5.5~11.2% larger than those for PF-5060 at the heat flux of $30W/cm^2$, and the local heat transfer coefficients reached an uniform value approximately after the fourth row, indicating that the thermally fully developed condition was reached after the fourth row.

(4) The present experimental data after the fourth row gave the best agreement with the values predicted by the Malina and Sparrow's correlation among several correlations, and the empirical correlations were obtained at the first, fourth, and sixth rows for a channel Reynolds number over 3,000.

References

Baker, E., 1972, "Liquid Cooling of Microelectronic Devices by Free and Forced Convection," *Microelectronics and Reliability*, Vol. 11, pp. 213~222.

Bar-Cohen, A., 1994, "Trends in the Packaging of Computer Systems," *In Cooling of Electronic Systems* (Edited by Kakac, C., Yuncu, H. and Hijikata, K.), Kluwer Academic Publishers, Dordrecht, pp. 17~45.

Bar-Cohen, A., 1997, "Recent Advances in Passive Immersion Cooling of High Power Devices," *Proceedings of the Pacific Rim/ASME International and Intersociety Electronic and Photonic Packaging Conference*, Hawaii, pp. 2053~2054.

Hartnett, J. P. Kostic, M., 1989, "Heat Transfer to Newtonian and Non-Newtonian Fluids in Rectangular Ducts," *Advances in heat transfer*, Vol. 19, pp. 247~356.

Heindel, T. J., Ramadhyani, S., Incropera, F. P., 1992, "Liquid Immersion Cooling of a Longitudinal Array of Discrete Heat Sources in Protruding Substrates: II-Forced Convection Boiling," *Trans. of the ASME, J. Electronic Packaging*, Vol. 114, pp. 63~70.

Incropera, F. P., 1988, "Convection Heat Transfer in Electronic Equipment Cooling," *Trans. of the ASME, J. Heat Transfer*, Vol. 110, pp. 1097~1111.

Incropera, F. P., Kerby, J. S., Moffatt, D. F., Ramadhyani, S., 1986, "Convection Heat Transfer from Discrete Heat Sources in a Rectangular Channel," *Int. J. Heat Mass Transfer*, Vol. 29, pp. 1051~1058.

Jones, Jr, O. C., 1976, "An Improvement in the Calculation of Turbulent Friction in Rectangular Ducts," *J. Fluid Engineering*, Vol. 98, pp. 173~181.

Malina, J. A. and Sparrow, E. M., 1964, "Variable Property, Constant Property and

Entrance Region Heat Transfer Results for Turbulent Flow of Water and Oil in a Circular Tube," *Chem. Eng. Sci.*, Vol. 19, pp. 953～962.

Moffat, R. J., 1985, "Using Uncertainty Analysis in the Planning of an Experiment," *J. Fluid Engineering*, Vol. 107, pp. 173～182.

Mudawar, I., Anderson, T. M., 1990, "Parametric Investigation into the Effects of Pressure, Subcooling, Surface Augmentation and Choice of Coolant on Pool Boiling in the Design of Cooling Systems for High Power Density Electronic Chips," *Trans. of the ASME, J. Electronic Packaging*, Vol. 112, pp. 357～382.

Mudawar, I., Maddox, D. E., 1990, "Enhancement of Critical Heat Flux from High Power Microelectronic Heat Sources in a Flow Channel," *Trans. of the ASME, J. Electronic Packaging*, Vol. 112, pp. 241～248.

Nakayama, W., 1997, "Liquid-cooling of Electronic Equipment: Where does it Offer Viable Solutions ?," *Proceedings of the Pacific Rim/ ASME International and Intersociety Electronic and Photonic Packaging Conference*, Hawaii, pp. 2045～2052.

Oskay, R. and Kakac, S., 1973, "Effect of Viscosity Variations on Turbulent and Laminar Forced Convection in Pipes," *METU J. Pure Applied Sci.*, Vol. 6, pp. 211～230.

Park, K. A., Bergles, A. E., 1987, "Natural convection heat Transfer Characteristics of Simulated Microelectronic Chips," *Trans. of the ASME, J. Heat Transfer*, Vol. 109, pp. 90～96.

Petukhov, B. S., 1970, "Heat Transfer and Friction in Turbulent Pipe Flow with Variable Physical Properties," *Advances in Heat Transfer*, Vol. 6, pp. 505～564.

Rogers, D. G., 1980, "Forced Convection Heat Transfer in Single Phase Flow of a Newtonian Fluid in a Circular Pipe," *CSIR Report CENG 322*, Pretoria, South Africa.

Sieder, E. N. and Tate, G. E., 1936, "Heat Transfer and Pressure Drop of Liquids in Tubes," *Ind. Eng. Chem.*, Vol. 28, pp. 1429～1453.